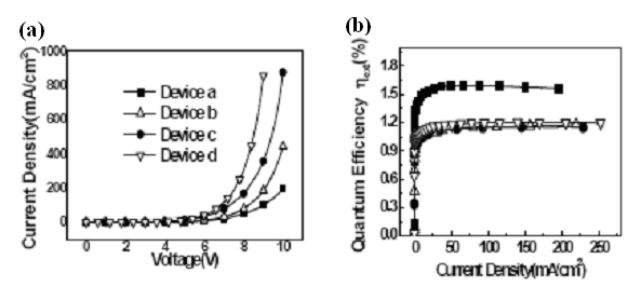
## Mechanisms of Enhanced Carrier Injection in Organic Light Emitting Devices

Chih-I Wu (吳志毅)<sup>1,2</sup>, Chang-Ting Lin (林昌廷)<sup>2</sup>, Yu-Hung Chen (陳裕宏)<sup>2</sup>, Mei-Hsin Chen (陳美杏)<sup>2</sup>, and Guan-Ru Lee (李冠儒)<sup>2</sup>

## <sup>1</sup>Department of Electrical Engineering, National Taiwan University, Taipei, Taiwan <sup>2</sup>Graduate Institute of Electro-optical Engineering, National Taiwan University, Taipei, Taiwan

The origins of barrier lowering leading to high efficient organic light emitting devices with incorporation of molybdenum oxide(MoOx) in anode structures are investigated. Ultraviolet and x-ray photoemission spectra reveal that p-type doping effects in the organic films and carrier concentration increase at the anode interfaces cause the hole injection barrier lowering. The gap states, which help carrier injection from the anodes, resulted from the oxygen deficiency in MoOx due to the interaction of organic materials and MoOx.

To compare with device performance, four sets of structures with device a, b, c and d are fabricated respectively. Device  $\mathbf{a}$ : ITO / m-MTDATA (30nm) / NPB(20nm) / Alq3 (60nm) / LiF (0.5nm) / Al (150nm), Device  $\mathbf{b}$ : ITO / MoO<sub>3</sub> (5nm) / NPB (45nm) / Alq3(60nm) / LiF (0.5nm) / Al (150nm), Device  $\mathbf{c}$ : ITO / MoO<sub>3</sub> (30nm) / NPB (20nm) / Alq3(60nm) / LiF (0.5nm) / Al (150nm), Device  $\mathbf{d}$ : ITO / MoO<sub>3</sub>: NPB (30nm, vol. 1:4) / NPB (20nm) / Alq3 (60nm) / LiF (0.5nm) / Al(150nm).



**Fig. 1:** (a) I-V characteristics, and (b) External quantum efficiency of devices with various HIL design based on structure B.

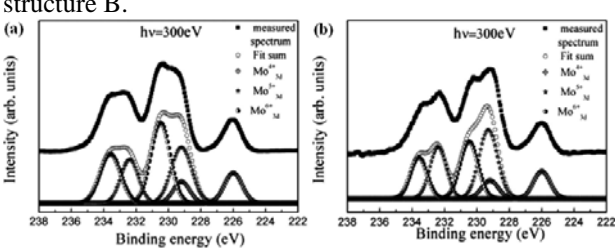


**Fig. 2:** (a) XPS Mo 3d core level spectra of pristine MoOx. (b) XPS Mo 3d core level of MoOx with a few angstroms of NPB deposition.

Figure 2 shows the XPS Mo 3d core-level spectra of  $MoO_3$  deposited on Au. The presence of mixed oxidation states of Mo are obviously deduced from the shape of XPS spectrum. We fit the spectrum with six overlapping Gaussian peaks which represent different oxidation states<sup>12,13</sup> of  $Mo^{4+}3d_{5/2}$ ,  $Mo^{5+}3d_{5/2}$ , and  $Mo^{6+}3d_{5/2}$ . When NPB deposits on  $MoO_3$ , it is apparent

that the increase of  $\mathrm{Mo^{5+}3d_{5/2}}$  states indicates the partial structure transition of  $\mathrm{MoO_3}$  to  $\mathrm{MoO_2}$ . Thus we can conclude the detailed interaction of  $\mathrm{MoO_3/NPB}$  interface.

The electronic properties and chemical interactions structures 4,7-diphenyl-1,10cathode using phenanthroline (Bphen) doped with rubidium carbonate (Rb<sub>2</sub>CO<sub>3</sub>) as electron injection layers were investigated. Current-voltage characteristics reveal that the devices with Bphen/Rb<sub>2</sub>CO<sub>3</sub> /Al as cathode structures possess better electron injection efficiency than those with cathode structures of Bphen/LiF/Al. Ultraviolet and xray photoemission spectroscopy shows that *n*-type doping effects resulting from Rb<sub>2</sub>CO<sub>3</sub> and the gap states created by aluminum deposition are both keys to the improved carrier injection efficiency. Moreover, theoretical calculation indicates that the chemical reaction between aluminum and the nitrogen atoms in Bphen is the origin of the gap states.

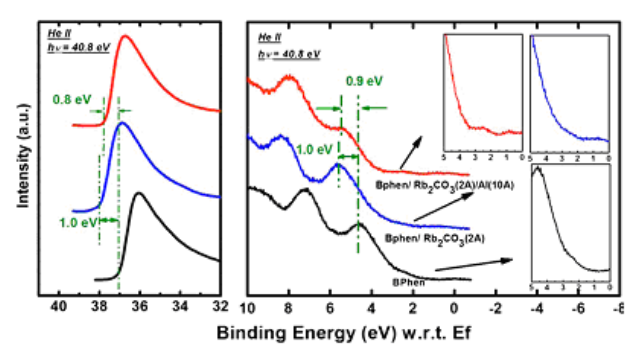


**Fig. 3:** UPS spectra, near the onset and valence bands, of Bphen with Rb<sub>2</sub>CO<sub>3</sub> and aluminum deposition.

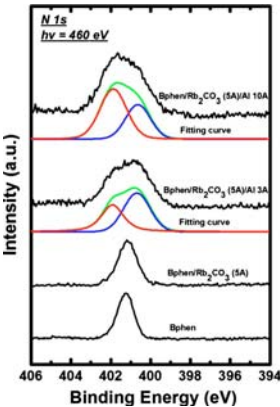


Fig. 4: XPS spectra of the nitrogen 1s core-level spectra of pristine Bphen with incremental depositions of Rb<sub>2</sub>CO<sub>3</sub> and aluminum.